Effects of Polymer Microenvironment on the Thermodynamics of the Twisted Intramolecular Charge Transfer Fluorescence

Shigeo Tazuke† and Rong Kun Guo*,[1]

Research Laboratory of Resources Utilization, Tokyo Institute of Technology, 4259 Nagatsuta, Midori-ku, Yokohama, Japan 227. *Received December 13, 1988; Revised Manuscript Received August 2, 1989*

ABSTRACT: The fluorescence behavior of poly(alkyl methacrylate)s (alkyl: methyl, butyl, cyclohexyl, and dodecyl) containing a trace amount of (dimethylamino)benzoate (DMAB) as fluorescence probe was investigated in different solvents (ethyl acetate, butyl chloride, and tetrahydrofuran) over the temperature range between −100 and 60 °C. For poly(methyl methacrylate) the activation energy (E_1) is almost constant in good solvents and comparable to or even less than the temperature dependence of solvent viscosity, suggesting that the molecular twisting motion is barrierless and the retarding effect of polymer chain is entropic. In poor solvents, an energy barrier owing to contracted polymer chain is particularly prominent when the probe is tagged to the polymer main chain via a long alkyl spacer. With increasing bulkiness of the ester alkyl group, E_1 tends to increase, reflecting the steric effect. Effects of bulky neighboring side groups (particularly in the case of poly(cyclohexyl methacrylate)) are prominent in poor solvents. The reverse reaction (i.e., regeneration of the local excited state (b*) from the a* state) was also found to be suppressed by the polymer chain. Temperature effects on TICT fluorescence were discussed in terms of solvation and excitation wavelength as well.

Introduction

Twisted intramolecular charge transfer (TICT) fluorescence has been proved to be an excellent probe to study polymer segment mobility. In a series of papers,[2-4] we have shown that the sidechain segment motions are controlled by the spacer distance to the main chain[3] and influenced strongly by the neighboring side chains in polymethacrylates having a variety of alkyl groups.[4] Furthermore, solvent effects controlling the main-chain conformation and consequently the segment mobility are very marked. Although it was possible to correlate the polymer effect on the fluorescence behavior to the chemical structure and chain conformation of the polymers,[5,6] the origin of polymer effects is not fully understood. For instance, the so-called polymer environmental effect may be attributed to steric factors retarding molecular motion[7] or to a change in solvation owing to the role of the polymer chain replacing the solvent molecules in the vicinity of the functional group of concern.[8] Such factors are not easily distinguished by measurements at a fixed temperature.

In addition, the kinetics of the TICT phenomenon initially proposed by Grabowski indicate that the relative intensity of TICT fluorescence (R) behaves very much like that of an excimer or an exciplex, showing a bell-shaped temperature dependence.[9,10] We have already shown that the temperature corresponding to the maximum R value shifts toward higher temperature when the TICT chromophore is bonded to poly(methyl methacrylate).[2] In the higher temperature side of T_{max}, the TICT excited state and the local excited state are in equilibrium and therefore the R value decreases with temperature. In the lower temperature side of T_{max}, the formation of the TICT state is a one way process with no reverse reaction, exhibiting a monotonic decrease of R value with decreasing temperature. In previous work,[2] we assumed that measurements at room temperature are in the low-temperature region so that the R value is a direct measure of the ease of generating a TICT state. This was confirmed for poly(methyl methacrylate) with a bonded DMAB group near the main chain but not for others.

With a series of samples having systematically modifed structures, it is appropriate to investigate temperature effects on TICT fluorescence. Temperature is one of the factors modulating the molecular environment without changing the chemical composition. Apparent results of the temperature variation study are obtained as $\Delta H^{\ddagger}$ and $\Delta S^{\ddagger}$. However, since the properties of the reaction medium such as viscosity and dielectric constant are dependent on temperature as well, the results obtained are complicated functions of the intrinsic thermodynamic activation parameters with additional contributions owing to changes in environmental factors. It is very difficult to distinguish these factors strictly, in particular with a single sample. By comparing a series of samples slightly different in chemical structure, it would be possible to discuss these various temperature-dependent factors.

Experimental Section

Sample preparation was already reported.[2-4] The structures and the abbreviations of all samples are shown in Scheme I.

Absorption spectra were recorded on a Hitachi UV-320 spectrophotometer. The corrected fluorescence spectra were recorded on a Hitachi MPF-4 spectrofluorometer under argon atmosphere in a sealed quartz cell. The polymer concentration is about 1% and the absorbance at 300 nm is about 0.15. Calibration and handling of the spectroscopic data were the same as reported. A cryostat (OXFORD Model DN1704) with its temperature controller (Model 3120) and a Yamato BH-71 thermocontrol unit were used for fluorescence measurement below and above room temperature, respectively. The temperature range covered was between −100 and 60 °C. The temperature was controlled within ±0.5 °C. Deterioration of sample during measurement was checked by absorption and fluorescence spectra. No deterioration was detected.

Results and Discussion

Brief Description of the Kinetic Scheme. The kinetic equations assuming stationary concentrations of the local excited state (b*) and the TICT state (a*) (Grabowski kinetic scheme[10,11]) and their application in polymeric systems have been described previously.[2] The

† Deceased on July 11, 1989.

0024-9297/90/2223-0719$02.50/0

Scheme I

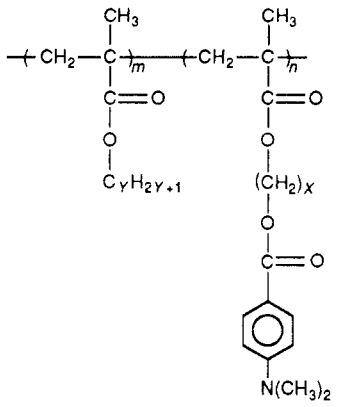

	Y	X	abbreviation
group A	1	2	poly(MMA-*co*-2)
	1	4	poly(MMA-*co*-4)
	1	8	poly(MMA-*co*-8)
	1	12	poly(MMA-*co*-12)
group B	4	12	poly(BMA-*co*-12)
	6[a]	12	poly(CHMA-*co*-12)
	12	12	poly(DDMA-*co*-12)

[a]For the cyclohexyl group, the number of Hs is 2*Y*.

equations necessary for the present discussion are given below.

fluorescence quantum yield of the a* emission

$$\phi_b = \frac{k_{bf}(k_2 + k_a)}{k_b(k_2 + k_a) + k_1 k_a} \quad (1)$$

fluorescence quantum yield of the a* emission

$$\phi_a = \frac{k_{af} k_1}{k_b(k_2 + k_a) + k_1 k_a} \quad (2)$$

$$R = \phi_a/\phi_b = \frac{k_{af} k_1}{k_{bf}(k_2 + k_a)} \quad (3)$$

Definitions of rate constants and symbols are as follows: k_1 is the forward rate constant of b* → a*, the activation energy being E_1. k_2 is the backward rate constant of b* ← a*, the activation energy being E_2. k_{af}^0 and k_{af}^1 are the rate constants for radiative transition from the a* state. Since the radiative transition from the vibrationally lowest a* state (k_{af}^0) is symmetry forbidden whereas that from the second lowest vibrationally excited state (k_{af}^1) is allowed, $k_{af}^1 > k_{af}^0$. Because the activation energy $h\nu_1$ is much smaller than E_1 ($h\nu_1$ is smaller by a factor of 10^{-2}–10^{-3}), we assume k_{af} to be independent of temperature relative to k_1: $k_{af} = k_{af}^0 + k_{af}^1 \exp(-h\nu_1/kT)$. $k_a = k_{af} + k_a^0$ where k_a^0 is the nonradiative rate constant from the a* state. $k_b = k_{bf} + k_b^0$ where k_{bf} and k_b^0 are the radiative and nonradiative rate constants from the b* state.

A measureable quantity is R given by (3). Since k_{af}, k_{bf}, and k_a are temperature independent, the temperature dependence of R is expressed by (4) and (5) for the low-temperature region (k_2 is negligible) and the high-temperature region (k_2 is not negligible), respectively.

$$R = C_1 \exp(-E_1/\kappa_B NT) \quad (4)$$

$$R = C_2 \exp(-E_2/\kappa_B NT) \quad (5)$$

κ_B is the Boltzmann constant.

General Trends of Polymer and Solvent Effects on TICT Phenomenon. Five sets of measurements shown in Figures 1 and 2 indicate that the polymer–solvent interaction reflects strongly the difference between polymers and the monomer model (BMABE). On comparison of Figure 1a with Figure 1b, EAc (Figure 1a) is a much better solvent than BuCl (Figure 1b) for PMMA. The polymer environmental effect is much larger in the latter solvent. The same is true for the set of poly(alkyl methacrylate)s shown in Figure 2. As indicated by the second virial coefficient A_2 values in Table II,[4] THF (Figure 2a) is a common good solvent for the four polymethacrylates with different ester alkyl groups whereas BuCl (Figure 2b) is a common poor solvent. The fluorescence behaviors in these two solvents are quite contrasting. While depression of the R value in these polymers relative to BMABE is moderate in THF, the difference between polymers and BMABE is drastic in BuCl. EAc (Figure 2c) is a good solvent for poly(BMA) but a poor solvent for poly(CHMA). This difference is explicitly shown in Figure 2c. These results are not unexpected from our previous discussions[3,4,7] that polymer chain conformation has critical effects on side-chain segment motion.

Although in the previous study the measurement was made at a fixed temperature (room temperature 20–25

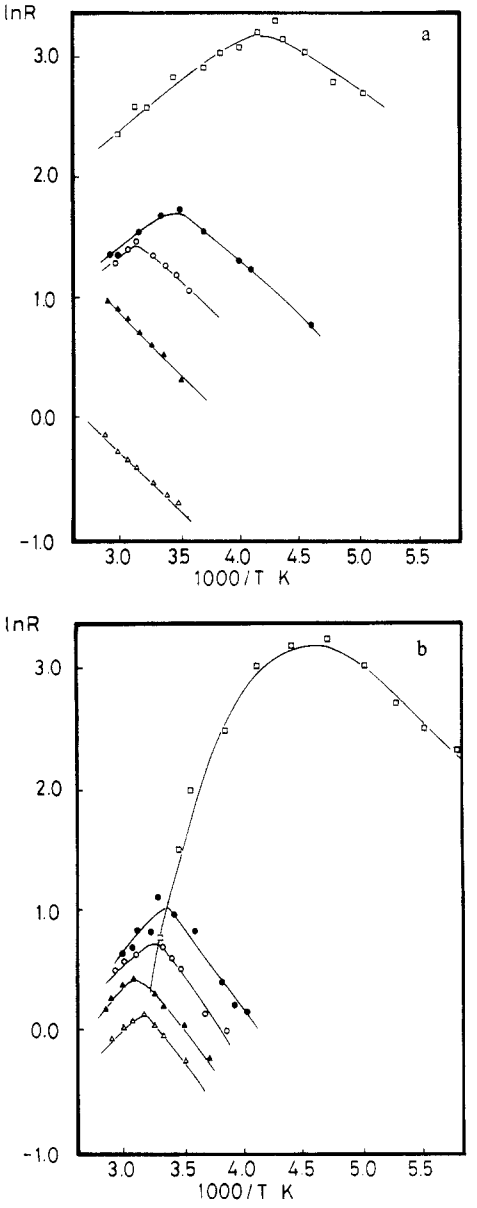

Figure 1. Temperature dependence of the emission intensity ratio R for poly(MMA-*co*-2) (△), poly(MMA-*co*-4) (▲), poly(MMA-*co*-8) (○), poly(MMA-*co*-12) (●) (1 wt %), and monomer model compound DMABE (□) (1×10^{-5} M) in EAc (a) and in BuCl (b). Excitation at 300 nm.

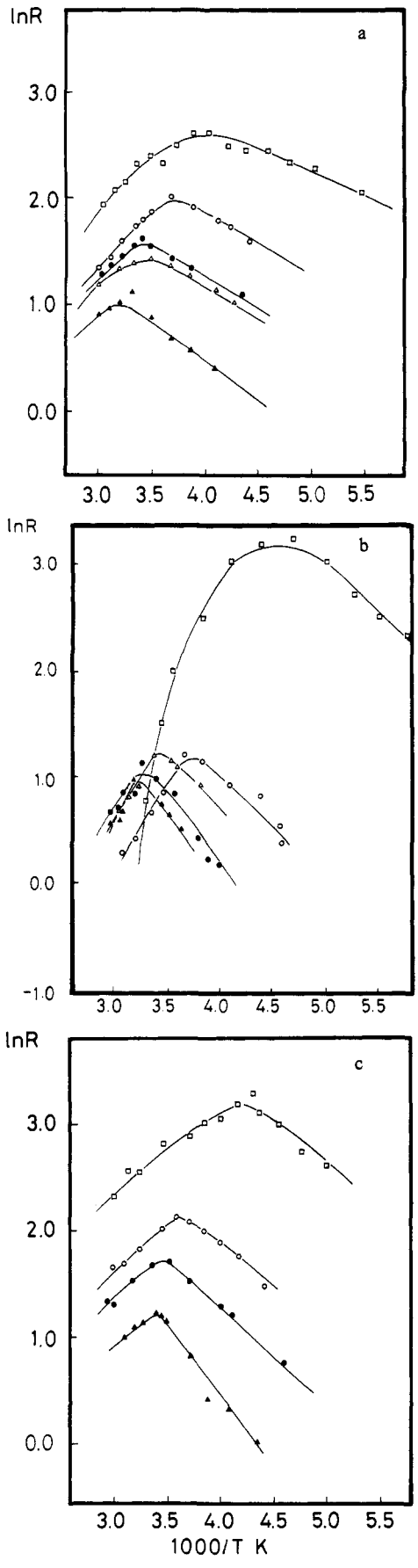

Figure 2. Temperature dependence of the emission intensity ratio R for poly(MMA-*co*-12) (●), poly(BMA-*co*-12) (○), poly(CHMA-*co*-12) (▲), poly(DDMA-*co*-12) (△) (1 wt %), and monomer model compound DMABE (□) (1×10^{-5} M) in THF (a), BuCl (b), and EAc (c). Excitation at 300 nm.

°C, $1/T = (3.41\text{–}3.36) \times 10^3$), the general conclusion that the R value is larger for the longer spacers and smaller for longer neighboring side chains is correct. The temperature range employed is in the critical zone where low-temperature behavior (exclusively b* → a* process) and high-temperature behavior (a* → b* process operative as well) cross. We employed the relative sequence of R values as a measure of the ease of segment rotational motion (i.e., b* → a*), which should in principle be determined at a much lower temperature. By a close look at the data in Figures 1 and 2, however, the sequence of R values at $1/T = 3.4 \times 10^3$ is unchanged in the low-temperature region except for BuCl (Figure 1b and Figure 2b). The temperature giving the maximum R value shifts irregularly from sample to sample in this poor solvent. In the following, we will discuss the results obtained mainly in the low-temperature region where the R values are more reliable than in the high-temperature region.

Activation Energy E_1 of TICT Formation. As shown in Figure 1a, the activation energy E_1 calculated as the slope of the Arrhenius plot of R in the low-temperature region[12] remains nearly constant despite the fact that the DMAB chromophore locates at a different distance from the PMMA main chain for each sample. EAc is a good solvent for PMMA as shown either by the exponential term α in the Sakurada–Mark–Houwink equation[13] or by the second virial coefficient A_2 determined by the light scattering method in our laboratory.[4]

The observed results are rather unexpected. The activation energy E_1 of TICT formation is almost independent of the spacer length connecting the DMAB group to the polymer main chain. Another important fact is that E_1 values for the polymers in the A group and DMABE (see Table I) are all smaller than the activation energy of solvent viscosity E_η. It has been reported for a typical TICT compound, 4-(*N*,*N*-dimethylamino)benzonitrile, that E_1 is related to the solvent viscosity but the value is smaller than E_η, indicating the b* → a* process to be virtually barrierless.[15,16]

There is a significant difference of $\sim 1.5 \times 10^2$ cm^{-1} in E_1 between DMABE and the polymers. This may suggest that there is a small energy barrier in the polymer system or the apparent E_1 is affected by the temperature-dependent polymer chain conformation. The R value tends to decrease with decreasing the solubilizing power of solvent as shown by smaller R values in BuCl. With decreasing temperature, polymer solubility decreases even in a good solvent. Consequently, the R value at lower temperature may be lowered as a result of polymer chain contraction. The apparent temperature dependence of the R value for polymers will therefore be higher than the true value.

Another set of approximately parallel Arrhenius plots of R is observed for the B group polymers in THF (Figure 2a). THF is a common good solvent for all poly(alkyl methacrylate)s used.[4] Since the E_1 values for these samples are smaller than E_η of THF (see Table II), the intramolecular potential barrier is absent in these cases as well. All data for group A and B polymers are summarized in Tables I and II, respectively.

In contrast to the data in a good solvent, EAC, in a poor solvent, BUCl,[3] the Arrhenius plots of group A polymers in the low-temperature region are no longer parallel with each other. The value $\Delta E_1 = E_1$(polymer) – E_1(BMABE) ranges from 1.0 for poly(MMA-*co*-2) to 2.7 $\times 10^2$ cm^{-1} for poly(MMA-*co*-12). This range is much wider than the corresponding value in EAc [(1.2–1.5) $\times 10^2$ cm^{-1}]. An additional energy barrier seems to increase

Table I
Temperature Dependence of R Values and Relevant Data for Group A Polymers[a]

sample	solvent	solvent E_T	E_1	ΔE_1[b]	E_2	T_{max}, K	R_{max}	ln $(R)_{1/T\to 0}$
DMABE	EAc	6.8	5.0		11.3	242–248	24.1	6.42
poly(MMA-*co*-12)			6.3	1.3	13.4	284–287	5.6	5.20
poly(MMA-*co*-8)			6.4	1.4	12.9	312–316	4.3	4.75
poly(MMA-*co*-4)			6.5	1.5		>333		4.35
poly(MMA-*co*-2)			6.2	1.2		>333		3.10
DMABE	BuCl	6.0	6.6			204–214	25.1	8.25
poly(MMA-*co*-12)			9.3	2.7	17.2	300–305	3.06	6.75
poly(MMA-*co*-8)			9.0	2.4	16.7	308–312	2.36	6.25
poly(MMA-*co*-4)			8.3	1.6	15.3	318–322	1.57	5.71
poly(MMA-*co*-2)			7.6	1.0	14.5	316–320	1.17	5.32

[a] All energies in 10^2 cm^{-1}. 1 kcal/mol = 3.5×10^2 cm^{-1}. [b] $\Delta E_1 = E_1$(polymer) − E_1 (DMABE).

Table II
Temperature Dependence of R Values and Relevant Data for Group B Polymers[a]

sample	solvent	solvent E_T	10^2A_2[b]	E_1	ΔE_1[c]	E_2	T_{max}, K	R_{max}	ln $(R)_{1/T\to 0}$
DMABE	THF	6.7		4.3		10.8	250–260	13.74	4.81
poly(MMA-*co*-12)			1.8	4.7	0.4	11.5	287–290	4.87	4.00
poly(BMA-*co*-12)			2.8	4.6	0.3	12.1	270–275	7.39	4.50
poly(CHMA-*co*-12)			3.2	5.4	1.1	11.6	300–302	2.85	3.70
poly(DDMA-*co*-12)			2.2	4.9	0.6	10.6	293–296	4.14	3.85
DMABE	BuCl	6.0		6.6			204–214	25.1	8.25
poly(MMA-*co*-12)			0.1	9.3	2.7	17.2	300–305	3.06	6.75
poly(BMA-*co*-12)			0.3	6.3	−0.3	18.8	285–288	3.67	5.81
poly(CHMA-*co*-12)			0.15	8.0	1.4	25.0	309–312	2.56	5.70
poly(DDMA-*co*-12)			0.2	6.4	−0.2	17.8	265–270	2.89	5.52
DMABE	EAc	6.8		5.0		11.3	242–248	24.1	6.42
poly(MMA-*co*-12)			4.3	6.3	1.3	13.4	284–287	5.6	5.20
poly(BMA-*co*-12)			8.5	5.6	0.6	12.0	280–283	8.40	5.80
poly(CHMA-*co*-12)			0.2	9.1	4.1	19.8	293–297	3.46	6.02

[a] All energies in 10^2 cm^{-1}. 1 kcal/mol = 3.5×10^2 cm^{-1}. [b] Second virial coefficient (see text). [c] $\Delta E_1 = E_1$(polymer) − E_1(DMABE).

Table III
Excitation Wavelength Dependence of Thermodynamic Parameters of TICT Formation for Poly(MMA-*co*-2) and Poly(CHMA-*co*-12) in EAc[a]

sample	excitation wavelength, nm	E_1, 10^2 cm^{-1}	ln $(R)_{1/T\to 0}$
poly(MMA-*co*-2)	290	6.51	2.12
	300	6.45	2.31
	310	6.28	2.60
	320	6.41	3.24
poly(CHMA-*co*-12)	290	9.26	4.98
	300	9.14	5.20
	310	9.88	5.38
	320	9.08	5.55

[a] 1 kcal/mol = 3.5×10^2 cm^{-1}.

along the reaction pathway from the b* state to the a* state with increasing spacer length in BuCl.[20] The sequence of ΔE_1 is the following: poly(MMA-*co*-12) > poly(MMA-*co*-8) > poly(MMA-*co*-4) > poly(MMA-*co*-2). An increase in ΔE_1 in BuCl with spacer length will be attributed to the steric factor brought about by contraction of the polymer chain in a poor solvent. Formerly we observed an increase in E_1 of poly(MMA-*co*-2) in EAc with increasing the polymer concentration beyond a critical concentration.[17] This phenomenon was interpreted as due to contraction of the mesh size[18] of the polymer chain with increasing polymer concentration. A shrunken polymer chain in BuCl is effective for increasing the energy barrier of rotation, particularly when the chromophore is exposed to the outside environment via a long spacer. The sequence of ΔE_1 shown above agrees with this discussion.

When the surrounding side chains become longer (group B polymers) and the chromophore is buried and therefore "protected" in the soft side chains, the effect of the poor solvent is greatly reduced (Table II). ΔE_1 values for poly(DDMA-*co*-12) and poly(BMA-*co*-12) are practically zero whereas that of poly(MMA-*co*-12) is 2.7×10^2 cm^{-1}.

Poly(CHMA-*co*-12) is a specific sample since this side group is rigid but rather small in length.[4] This is probably the reason for the relatively high value of ΔE_1 of this sample in both a good solvent (THF) and poor solvents (EAc and BuCl).

It is rather surprising that the polymer effect is mostly attributed to the preexponential factor for group A polymers.

Preexponential Factor of TICT Formation. The preexponential factor, C_1 in (4), for the b* → a* process was estimated. The preexponential factor relative to that of BMABE was plotted in Figure 3 as a function of the spacer length for group A polymers. While C_1 includes all temperature-independent rate constants (k_{af}, k_{bf}, and k_a), there are all unimolecular rate constants and insensitive to molecular environment. In the following discussion, we assume that these rate constants are not affected by polymer structure.

The unfavorable preexponential factor for group A polymers may be interpreted as follows. In the polymers represented by poly(MMA-*co*-2), the number of available sites to accommodate the polar TICT state will be limited because solvation in the vicinity of polymer chain is restricted. We have several pieces of evidence that the restructuring of the polymer environment to an instantaneously produced polar excited state is slow.[7,19] We observed a time-dependent red shift of exciplex emission on the nanosecond time scale, whereas no such shift was detected in the small molecular model system.[20] In the experiment employing intramolecular exciplex formation with 1-(1-pyrenyl)-3-(4-(*N*,*N*-dimethylamino)-phenyl)propane as a fluorescence probe to monitor molec-

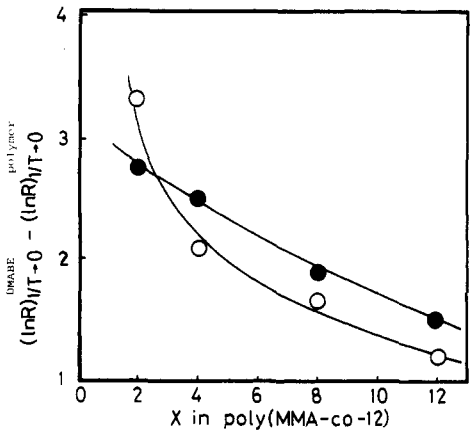

Figure 3. Relative decrease in ΔS^* for DMABE using that of poly(MMA-*co*-12) as a function of the carbon number X in the spacer length.

ular mobility, the rate of exciplex formation of the probe bonded to the PMMA side chain in dilute solution is also much slower than that of the reference monomer model system.[7]

It is a delicate question whether the entropically unfavorable TICT state formation in the polymer is due directly to slow segment motion in the polymer or attributable to restricted restructuring of the molecular encironment including solvation. Although we cannot provide a definite answer, the recent results of a time-resolved study on the solvation dynamics of the charge-transfer state of bis[4-(dimethylamino)phenyl]sulfone suggest solutions. The dynamics is dependent on restructuring of the surrounding medium.[21] When the restructuring delays and therefore the a* state is not accommodated instantaneously, the probability of forming the TICT state will be reduced.

The general conclusion concerning the importance of the preexponential factor is also acceptable for group B polymers (Figure 2). However, the polymer–solvent interaction changes from sample to sample, which makes discussion complicated. For example, the sequence of Arrhenius plots in Figure 2a is confusing unless we admit that poly(BMA-*co*-12) has a better solubility than poly(MMA-*co*-12) in THF.[4]

Equilibrium Temperature T_{max} and TICT Phenomenon in the High-Temperature Region. From the analysis of the TICT kinetics in the high-temperature region together with the low-temperature behavior, we could derive total kinetic parameters for both forward and backward processes. As shown in Figures 1 and 2, some of the measurements in the high-temperature region are less accurate because of the limited temperature range of measurement. In Figure 1a, we cannot observe T_{max} for poly(MMA-*co*-4) and poly(MMA-*co*-2). In Figure 1b, the shape of the Arrhenius plot for DMABE in the high-temperature region is not straight and furthermore the temperature range of measurement is very narrow for polymers. For Figure 2a,b, some samples could not be measured properly as well. Figure 2c provides the clearest data. Because of these difficulties, we discuss only the general trend in the high-temperature region.

Figure 1a shows that T_{max}, at which R reaches the maximum value R_{max}, shifts toward higher temperature when the spacer length becomes shorter. For poly(MMA-*co*-2) and poly(MMA-*co*-4), T_{max} is higher than 60 °C, which is above the temperature region of measurement. T_{max} of polymers with different side chains seems to be determined by the balance between the size of side chains and the conformation of the polymer chain (Figure 2).

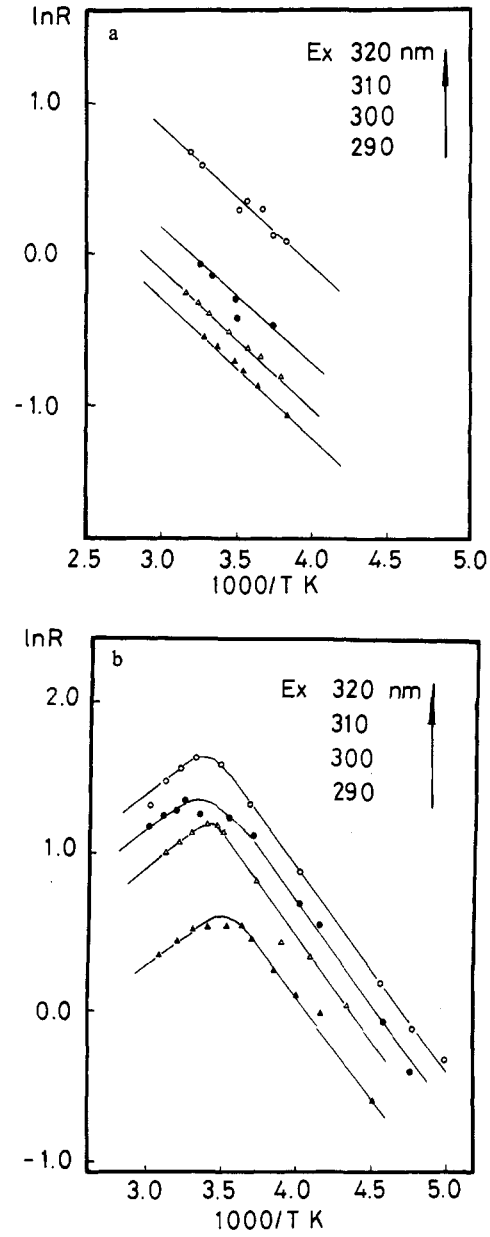

Figure 4. Temperature dependence of the emission energy of the TICT a* state for poly(MMA-*co*-2) (●), poly(MMA-*co*-12) (○), and DMABE (△) in EAC (a) and in BuCl (b), the concentration is as the above.

Because T_{max} is known to be determined by the competition between k_2 and k_a^0,[16,22] the present result implies that k_2 is strongly controlled as well by polymer structure. k_2 decreases with decreasing spacer length connecting the DMAB group to the main chain or increasing bulkiness of the adjacent side chains. We can therefore draw a picture that a polymer with slow formation of the a* state is also slow to regenerate the b* state from the a* state. Correlation between the magnitudes of E_1 and E_2 can also be seen. Both E_1 and E_2 for poly(CHMA-*co*-12) are much larger than those for other samples in BuCl as well as in EAc (Table II).

Effects of the Excitation Wavelength on the Shape of the Arrhenius Plots. Under the condition of restricted molecular mobility, the relative intensity of the a* band to the b* band often depends on the wavelength of excitation. When the red edge of the absorption band is excited, the intensity of the a* band is enhanced. This effect called the red-edge excitation (REE)[23,24] effect was found in dilute fluid solutions of the present poly-

mers.[3,4] When conformational motion is restricted, a number of conformers absorbing at different wavelengths are considered to be independent of each other within the time scale of the excited-state lifetime. By excitation at the red edge, the conformers having partially twisted structures in the ground state are excited and undergo more facile conversion to the a* state since the necessary angle of rotation is smaller.

The magnitude of REE also depends on the distance of the chromophore from the polymer main chain and the bulkiness of the neighboring side chains. Poly(MMA-*co*-2) and poly(CHMA-*co*-12) have been found to have the largest REE effect in the A and B groups,[3,4] respectively. It is interesting to examine whether REE facilitates TICT phenomenon enthalpically or entropically. Figure 4 shows the Arrhenius plots with varying wavelength of excitation.

As clearly shown in Figure 4, the changes in the excitation wavelength do not affect the slope of the Arrhenius plots; the origin of the REE effect is attributed to the temperature-independent term. The results are in accordance with the previous discussion that the b* → a* process is a barrierless process. Even if the ground-state conformation is partially twisted, a difference appears only in the probability and not in the enthalpy term of producing the perpendicularly twisted TICT state.

Conclusion

Polymer environmental effects on the TICT phenomena are mostly attributed to entropy effects. In comparison with small molecular model compounds, TICT formation in polymer-bound systems is not enthalpically favorable, but the effect is rather small except for the case where the chromophore is supposed to interact with contracted polymer chains in poor solvents. The entropically unfavorable TICT phenomena in polymers are probably related to the reduced number of solvation sites in polymeric systems. Direct determination of the rate of formation of the a* state will provide a clearer picture than the discussion based on stationary fluorescence spectroscopy. Rise and decay measurements of the a* band in the picosecond time range are now under way.

Acknowledgment. We thank Dr. R. Hayashi for his computer program separating the dual fluorescence bands and Dr. N. Kitamura and H. B. Kim for their helpful discussion.

References and Notes

(1) Visiting fellow from the Institute of Photographic Chemistry, Academia Sinica, Beijing, China.
(2) Hayashi, R.; Tazuke, S.; Frank, C. W. *Macromolecules* **1987**, *20*, 983.
(3) Tazuke, S.; Guo, R. K.; Hayashi, R. *Macromolecules* **1988**, *21*, 1046.
(4) Tazuke, S.; Guo, R. K.; Hayashi, R. *Macromolecules* **1989**, *22*, 729.
(5) Guillet, J. E. *Polymer Photophysics and Photochemistry*; Cambridge University Press: Cambridge, 1985.
(6) Winnik, M. A., Ed. *Photophysical and Photochemical Tools in Polymer Science*; Reidel: Dordrecht, Netherlands, 1987.
(7) Tazuke, S.; Iwasaki, R. *Japan-US Polym. Symp. Kyoto* **1985**, *Oct.* Preprints 199.
(8) Okata, T.; Fujita, T.; Mataga, W. *Z. Phys. Chem. N. F.* **1976**, *101*, 57.
(9) Grabowski, Z. R.; Rotkiewicz, K.; Rubaszeska, W.; Kirkor-Kaminska, E. *Acta Phys. Pol.* **1978**, *A54*, 767.
(10) Rettig, W. *Angew. Chem.* **1986**, *98*, 969; *Angew. Chem. Int. Ed. Engl.*; **1986**, *25*, 971.
(11) Grabowski, Z. R.; Dobkowski, J. *Pure Appl. Chem.* **1983**, *55*, 245.
(12) Strictly, the slope of the Arrhenius plot in the low-temperature region consists of the sum of E_1 and the energy gap between the lowest and the second lowest vibration levels ($h\nu_1$). If the contribution of $h\nu_1$ is not neglected, the activation energy barrier is even smaller than the values in Table I.
(13) *Polymer Handbook*, 2nd ed.; Brandrup, J., Immergut, E. H., Eds.; Wiley Interscience: New York, 1970.
(14) The E_η values were calculated by plotting the viscosity data obtained by the improved van Velzen–Cardozo–Langenkamp formula as a function of temperature (*The Properties of Gases and Liquids*; Reid, R. C., Prausnitz, J. M., Sherwood, T. K.; McGraw-Hill Inc.: New York, 1977; p 627): $\log(\eta) = (\text{vis } B)(1/T - (1/\text{vis } T_0)$, where vis B and vis T_0 are empirical parameters. The applicable temperature range is from 20 to 30 °C above freezing point to $T_r \sim 0.75(T_r = T/T_c)$, which is wide enough for the present discussion. It seems to be questionable whether macroscopic viscosity based on translational molecular motion can be quantitatively related to the friction of molecular rotation.
(15) Lippert, E.; Rettig, W.; Bonacic-Koutecky, V.; Heisel, F.; Hiehe, J. A. *Adv. Chem. Phys.* **1987**, *68*, 1.
(16) Rettig, W. *J. Lumin.* **1980**, *26*, 21.
(17) Hayashi, R.; Tazuke, S.; Frank, C. W. (a) *Photophysics of Polymer*; ACS Symposium Series 358; American Chemical Society: Washington, DC; 1987; p 135; (b) *Chem. Phys. Lett.* **1987**, *20*, 983.
(18) de Gennes, P.-C. *Scaling Concepts in Polymer Physics*; Cornell University Press: London, 1979.
(19) Tazuke, S. *Makromol. Chem. Suppl.* **1985**, *14*, 145.
(20) Tazuke, S.; Higuchi, Y.; Tamai, No.; Kitamura, N.; Tamai, Na.; Yamazaki, I. *Macromolecules* **1986**, *19*, 603.
(21) (a) Simon, J. D. *Acc. Chem. Res.* **1988**, *21*, 128. (b) Simon, J. D.; Su, S. G. *J. Chem. Phys.* **1987**, *87*, 7016. (c) Su, S. G. *J. Phys. Chem.* **1987**, *91*, 2693.
(22) Rettig, W.; Wermuth, G. *J. Photochem.* **1985**, *28*, 351.
(23) Al-Hassan, K. A.; El-Bayoumi, M. A. *Chem. Phys. Lett.* **1980**, *76*, 120.
(24) Al-Hassen, K. A.; Rettig, W. *Chem. Phys. Lett.* **1986**, *126*, 273.